Internal Coupled-Fed Dual-Loop Antenna Integrated With a USB Connector for WWAN/LTE Mobile Handset

Fang-Hsien Chu, *Student Member, IEEE*, and Kin-Lu Wong, *Fellow, IEEE*

***Abstract*—A coupled-fed dual-loop antenna capable of providing eight-band WWAN/LTE operation and suitable to integrate with a USB connector in the mobile handset is presented. The antenna integrates with a protruded ground, which is extended from the main ground plane of the mobile handset to accommodate a USB connector functioning as a data port of the handset. To consider the presence of the integrated protruded ground, the antenna uses two separate shorted strips and a T-shape monopole encircled therein as a coupling feed and a radiator as well. The shorted strips are short-circuited through a common shorting strip to the protruded ground and coupled-fed by the T-shape monopole to generate two separate quarter-wavelength loop resonant modes to form a wide lower band to cover the LTE700/GSM850/900 operation (704–960 MHz). An additional higher-order loop resonant mode is also generated to combine with two wideband resonant modes contributed by the T-shape monopole to form a very wide upper band of larger than 1 GHz to cover the GSM1800/1900/UMTS/LTE2300/2500 operation (1710–2690 MHz). Details of the proposed antenna are presented. For the SAR (specific absorption rate) requirement in practical mobile handsets to meet the limit of 1.6 W/kg for 1-g human tissue, the SAR values of the antenna are also analyzed.**

***Index Terms*—Coupled-fed loop antennas, handset antennas, LTE antennas, mobile antennas, USB connector, WWAN antennas.**

I. Introduction

SEVERAL internal mobile handset antennas capable of covering eight-band WWAN/LTE operation in the 704–960 and 1710–2690 MHz bands have recently been demonstrated [1]–[8]. In order to provide wideband operation and low SAR (specific absorption rate) values to meet the limit of 1.6 W/kg for 1-g head tissue [9], these WWAN/LTE handset antennas are generally disposed on the no-ground portion at the entire bottom edge of the system circuit board [8], [10]–[13]. In this case, the integration of such an antenna with nearby electronic elements such as a USB (universal series bus) connector [14]–[16], which is usually mounted at the bottom edge of the handset and used as a data port for external devices, becomes a challenging problem. This is because the presence of the USB connector, which is a conducting object, is generally not considered in the antenna design. Hence, when the USB connector is placed very close to the antenna, some undesired coupling will usually occur to cause degrading effects on the impedance matching of the antenna, thereby greatly decreasing the bandwidth of the antenna. Many traditional internal WWAN handset antennas [17]–[23] also have a similar problem, which causes a limitation in achieving compact integration of the internal antenna with associated electronic elements inside the handset.

To overcome the problem, we present in this paper a promising coupled-fed dual-loop handset antenna to integrate with a USB connector (typical size $9 \times 7 \times 4$ mm^3 for mini USB connector [14]) and cover eight-band WWAN/LTE operation which includes the LTE700/GSM850/900 bands (704–787/824–894/880–960 MHz) and the GSM1800/1900/UMTS/LTE2300/2500 bands (1710–1880/1850–1990/1920–2170/2300–2400/2500–2690 MHz). The antenna is mounted above a protruded ground extended from the main ground plane of the handset, while there is a USB connector mounted on the protruded ground. The antenna is further short-circuited to the protruded ground, and the presence of the USB connector on the protruded ground is included in the antenna design. Details of the proposed antenna are described in the paper. With the presence of the protruded ground below the antenna, the design considerations for achieving two wide operating bands to cover the desired 704–960 and 1710–2690 MHz bands are addressed. A parametric study of the major parameters of the antenna is also conducted. The obtained results including the antenna's radiation characteristics and its SAR values for 1-g head tissue are also presented.

II. Proposed Antenna

Fig. 1(a) and (b) shows the geometry of the proposed coupled-fed dual-loop mobile handset antenna integrated with a USB connector. Detailed dimensions of the antenna's metal pattern are shown in Fig. 1(c). Note that a USB connector is mounted on the protruded ground of size 10×10 mm^2 extended from the main ground plane of size 55×105 mm^2. The protruded ground and main ground plane are both printed on the back surface of a 0.8-mm thick FR4 substrate of size 55×115 mm^2, relative permittivity 4.4 and loss tangent 0.02 in the study, which is treated as the main circuit board of a practical smartphone. The selected dimensions of the main circuit board are reasonable for practical smartphones.

The antenna is centered above the protruded ground. A meandered shorting strip of length 17.8 mm and width 0.5 mm (section BB′) short-circuits the antenna to the protruded ground. The short-circuiting integrates the USB connector mounted on the protruded ground with the antenna. Further, by using a meandered shorting strip, additional inductance is expected to be

Manuscript received January 05, 2011; revised March 21, 2011; accepted April 30, 2011. Date of publication August 12, 2011; date of current version November 02, 2011.

F.-H. Chu and K.-L. Wong are with the Department of Electrical Engineering, National Sun Yat-sen University, Kaohsiung 80424, Taiwan (e-mail: wongkl@mail.nsysu.edu.tw).

Color versions of one or more of the figures in this paper are available online at http://ieeexplore.ieee.org.

Digital Object Identifier 10.1109/TAP.2011.2164220

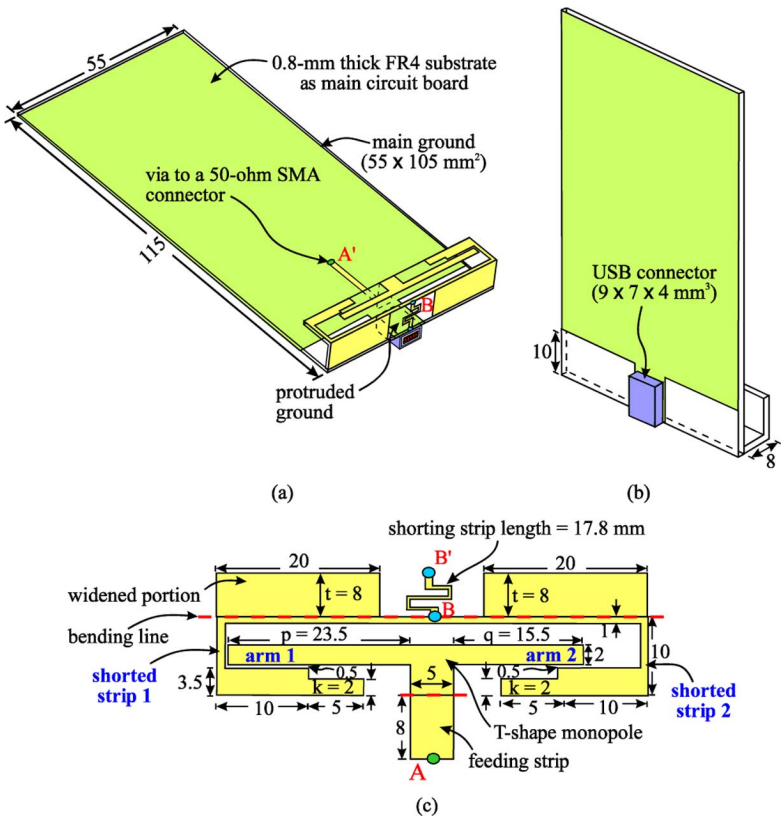

Fig. 1. (a) Geometry of the proposed coupled-fed dual-loop mobile handset antenna integrated with a USB connector. (b) A USB connector mounted on the protruded ground. (c) Dimensions of the antenna's metal pattern.

contributed to the antenna's input impedance. This causes shifting of the excited resonant modes to lower frequencies, which is helpful in achieving decreased size of the internal antenna for eight-band WWAN/LTE operation.

To achieve two wide operating bands for the desired WWAN/LTE operation, the antenna is composed of two separate shorted strips and a T-shape monopole encircled therein as a coupling feed and a radiator as well. The two shorted strips (strip 1 and 2) are of the same dimensions and are short-circuited to the protruded ground through the meandered shorting strip. Each arm (arm 1/arm 2) of the T-shape monopole couples to the open end of each shorted strip (strip 1/strip 2) through a coupling gap of 0.5 mm. By tuning the length p and q of the two arms (one is 23.5 mm and the other is 15.5 mm), two separate quarter-wavelength loop resonant modes can be excited to form a wide lower band to cover the desired 704–960 MHz band. With the successful excitation of the quarter-wavelength loop resonant mode [11], [24], which is different from the traditional internal loop handset antennas operated at the half-wavelength resonant mode as the fundamental or lowest-frequency mode [25]–[31]. This leads to the size reduction of the internal loop handset antennas for the WWAN/LTE operation.

By adjusting the width k ($k = 2$ mm in the proposed design) of the open-end sections of the two shorted strips, improved impedance matching of the excited resonant modes, especially the quarter-wavelength loop resonant modes, of the antenna can also be obtained. Further, an additional higher-order loop resonant mode is generated to combine with two wideband resonant modes contributed by the T-shape monopole [32] to form a very wide upper band of larger than 1 GHz to cover the desired 1710–2690 MHz.

Note that in order to enhance the operating bandwidth, there are widened portions (width $t = 8$ mm) in the two shorted strips. The widened portions and the meandered shorting strips are disposed on a 0.8-mm thick FR4 substrate of size 8×55 mm^2 and placed orthogonal to the edge of the main circuit board. Strip 1 and 2 and T-shape monopole, except a portion (length 8 mm and width 5 mm) of the central arm as the antenna's feeding strip made by a 0.2-mm thick copper plate, are disposed on a 0.8-mm thick FR4 substrate of size 10×55 mm^2 and placed parallel to the protruded ground. The front end (point A) of the feeding strip is the antenna's feeding point, which is connected to a 50-Ω microstrip feedline of length 20 mm printed on the front surface of the main circuit board. In the experiment for testing the fabricated antenna (see photos in different views shown in Fig. 2), the microstrip feedline is further connected through a via-hole to a 50-Ω SMA connector mounted on the back surface of the main circuit board.

III. Results and Discussion

Based on the dimensions given in Fig. 1, the antenna was fabricated as shown in Fig. 2. Fig. 3 shows the measured and simulated return loss for the antenna. The simulated results are obtained using HFSS (high frequency structure simulator) version 12 [33], and agreement between the measured data and simulated results is seen. Two wide operating bands have been obtained for the antenna. The lower band is formed by two resonant modes which are contributed by the two coupled-fed loop resonant paths provided by the antenna. Based on the bandwidth definition of 3:1 VSWR (6-dB return loss) [34]–[36], which is widely used as the design specification of the internal

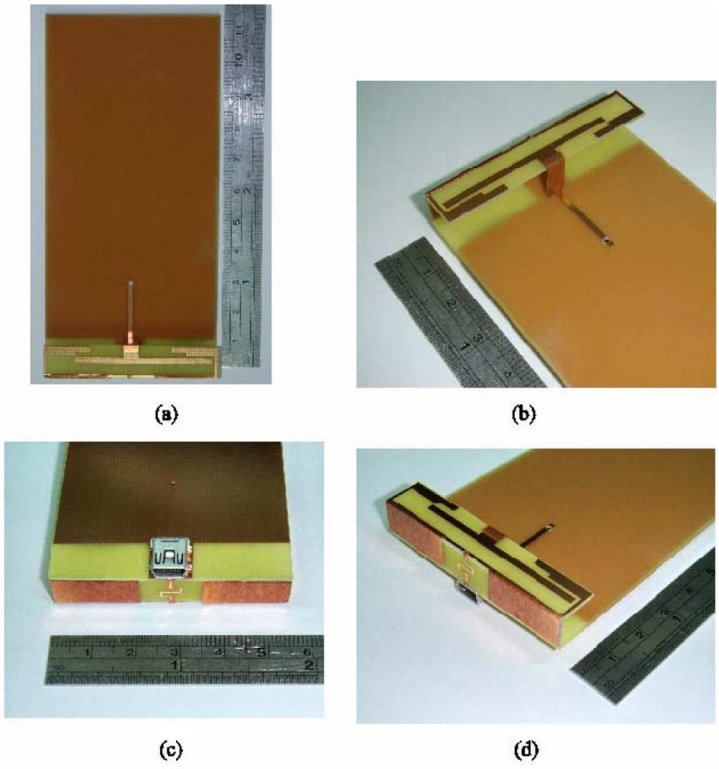

Fig. 2. Photos of the fabricated antenna in different views. (a) Front view. (b) Front view seeing the complete T-shape monopole. (c) Back view seeing the USB connector on the protruded ground. (d) Front view seeing the widened portion and USB connector.

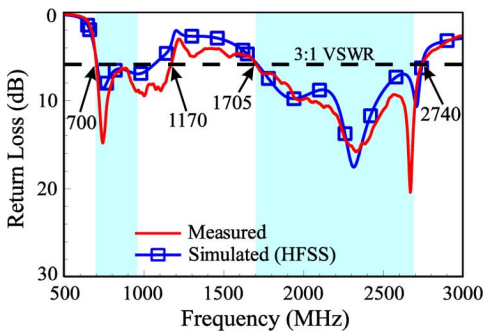

Fig. 3. Measured and simulated return loss for the proposed antenna.

WWAN/LTE handset antenna, the lower band covers the desired 704–960 MHz band. The upper band is formed by three resonant modes and shows a bandwidth of larger than 1 GHz to cover the desired 1710–2690 MHz band.

Fig. 4 shows the measured three-dimensional (3-D) total-power and two-dimensional (2-D) radiation patterns at typical frequencies. Note that the antenna is mounted at the bottom of the main circuit board. The 2-D radiation patterns are shown in three principal planes, and the normalization for the field strengths in the three planes is the same. At 740 and 925 MHz, dipole-like radiation patterns are observed, and omnidirectional radiation in the azimuthal plane (x–y plane) is seen. For higher frequencies at 1795, 1920 and 2350 MHz, relatively large variations in the radiation patterns are seen. The obtained radiation patterns are similar to those of many reported internal WWAN handset antennas [3], [4]. Fig. 5 shows

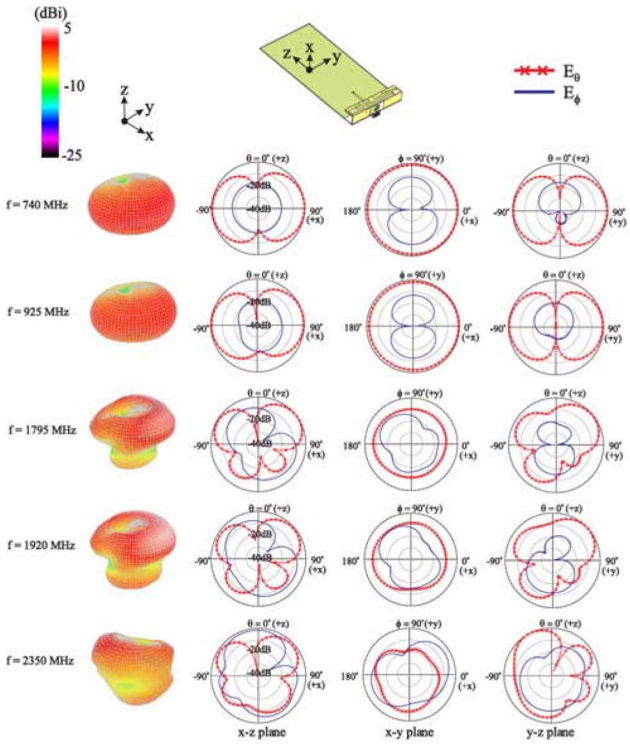

Fig. 4. Measured three-dimensional (3-D) total-power and two-dimensional (2-D) radiation patterns for the proposed antenna.

the measured antenna efficiency (mismatching loss included) for the proposed antenna. Results are measured in a far-field anechoic chamber. The measured radiation efficiency is about

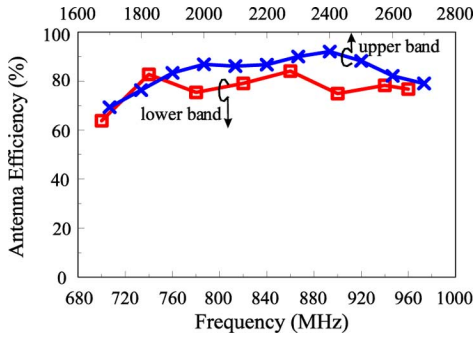

Fig. 5. Measured antenna efficiency (mismatching loss included) for the proposed antenna.

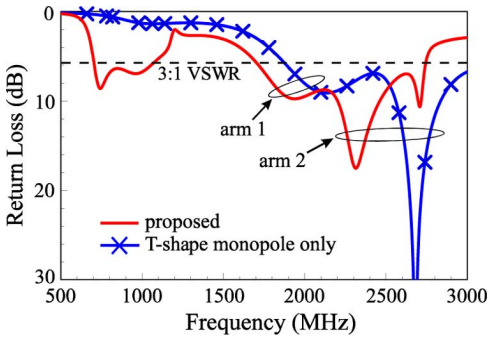

Fig. 6. Simulated return loss for the proposed antenna and the case with the T-shape monopole only.

63–83% for the lower band and about 70–91% for the upper band, which are good for practical mobile phone applications.

In the following, details of the operating principle of the antenna and the excited resonant modes are discussed in Figs. 6 and 7. A parametric study of the major design dimensions is analyzed in Figs. 8–11. Fig. 6 shows the simulated return loss for the proposed antenna and the case with the T-shape monopole only. It is seen that without the two shorted strips, the lower band cannot be excited. On the other hand, a wide operating band formed by two resonant modes (the first one at about 2.15 GHz contributed by arm 1 and the second one at about 2.7 GHz contributed by arm 2) is obtained for the case with the T-shape monopole only. This indicates that the T-shape monopole is also an efficient radiator in the proposed antenna.

The simulated return loss for the proposed antenna and the case with the coupled-fed loop on the left-hand side (arm 1 and shorted strip 1) only is also shown in Fig. 7. It is seen that only a resonant mode is excited at about 800 MHz and is far from covering the desired lower band. An additional resonant mode at about 2.7 GHz, which is a higher-order mode contributed by shorted strip 1, is excited to enhance the bandwidth of the antenna's upper band. It is also noted that when arm 2 is not present, the second resonant mode in the antenna's upper band cannot be excited.

A parametric study of the major design dimensions of the antenna is also analyzed. Fig. 8(a) shows the simulated return loss as a function of the length p of arm 1. Other dimensions are the same as in Fig. 1. Results for the length p varied from 19.5 to 23.5 mm are presented. It is seen that the first resonant mode in the antenna's upper band shifts to lower frequencies with

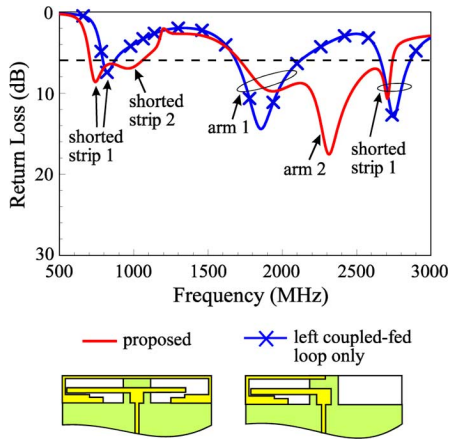

Fig. 7. Simulated return loss for the proposed antenna and the case with the coupled-fed loop on the left-hand side (arm 1 and shorted strip 1) only.

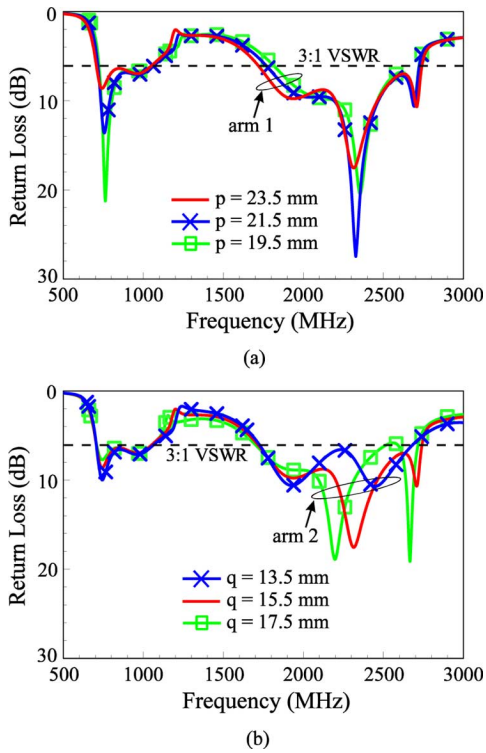

Fig. 8. Simulated return loss as a function of (a) the arm length p and (b) the arm length q of the T-shape monopole. Other dimensions are the same as in Fig. 1.

an increase in the length p. This behavior is reasonable since this resonant mode is mainly contributed by arm 1. In addition, since arm 1 affects the coupling between the T-shape monopole and the shorted strips, some variations in the impedance matching of the antenna's lower band are seen. The results for the length q of arm 2 varied from 13.5 to 17.5 mm are presented in Fig. 8(b). Large effects on the second resonant mode in the antenna's upper band, which is mainly contributed by arm 2, are seen. Similarly, since arm 2 affects the coupling between the T-shape monopole and the shorted strips, some variations in the impedance matching of other excited resonant modes can be seen. Also, larger effects of the length q of arm 2 than the length p of arm 1 on the frequency shifts of their respective

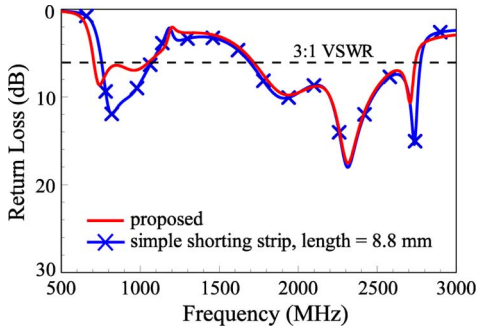

Fig. 9. Simulated return loss for the proposed antenna and the case with a simple linear shorting strip of length 8.8 mm. Other dimensions are the same as in Fig. 1.

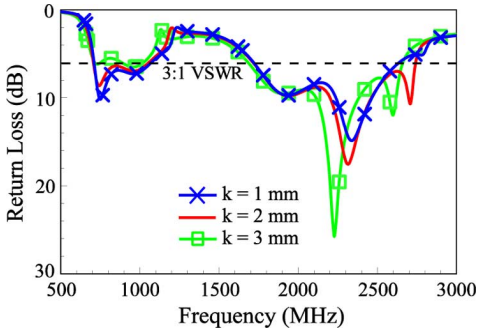

Fig. 10. Simulated return loss as a function of the open-end width k of the shorted strips. Other dimensions are the same as in Fig. 1.

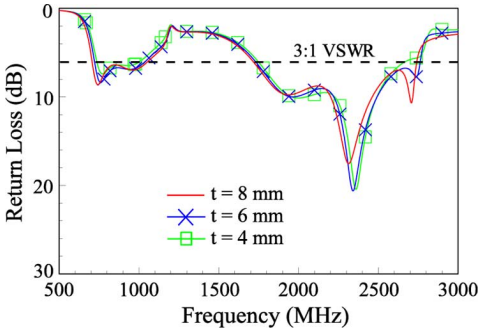

Fig. 11. Simulated return loss as a function of the width t of the widened portions. Other dimensions are the same as in Fig. 1.

contributed resonant modes are probably because arm 2 has a shorter length than arm 1, and hence the same length variation will cause larger frequency shift seen in Fig. 8(b). In addition, since arm 2 is shorter than arm 1, larger coupling variations for a same length variation can be expected (see related discussions in Fig. 10), which is also expected to result in larger frequency shift seen in Fig. 8(b). The results shown in Fig. 8(a) and (b) confirm that the first two resonant modes in the upper band are contributed by the T-shape monopole and can be adjusted by tuning the length p and q of arm 1 and 2.

Fig. 9 shows the simulated return loss for the proposed antenna and the case with a simple linear shorting strip of length 8.8 mm. Shifting of the antenna's lower band to lower frequencies is achieved by using the meandered shorting strip to replace the simple shorting strip. This is mainly because the meandered shorting strip can lead to a longer loop resonant path, hence resulting in the lowering of the excited loop resonant modes.

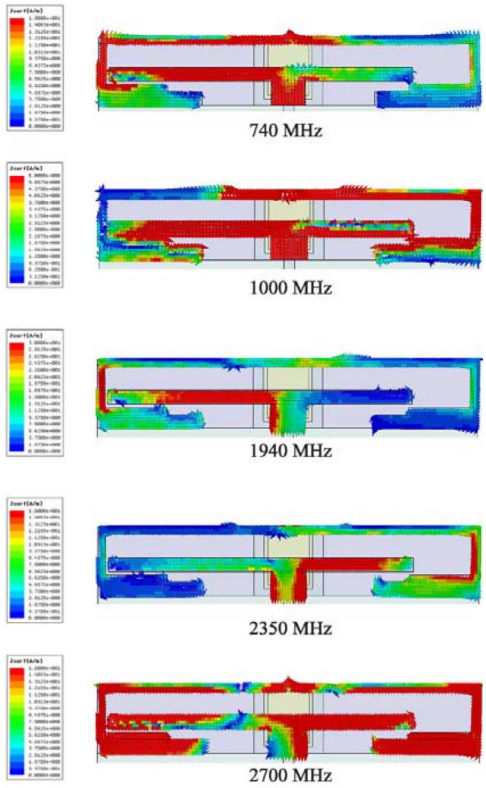

Fig. 12. Simulated surface current distributions on the major metal pattern of the antenna.

Effects of the open-end section of the shorted strips are also studied. Results of the simulated return loss of the open-end width k varied from 1 to 3 mm are shown in Fig. 10. Since the open-end width can adjust the coupling between the T-shape monopole and the shorted strips, large effects on the loop resonant modes are seen. Also, large effects on the second mode in the upper band, which is mainly contributed by arm 2, are seen. This behavior is largely because arm 2 has a shorter length than arm 1, and hence the coupling variations caused by the variations in the width k will be larger for arm 1. Thus, the variations in the width k will lead to large effects on the resonant mode contributed by arm 2.

Effects of the widened portions in the shorted strips are also analyzed. Fig. 11 shows the simulated return loss for the width t of the widened portions varied from 4 to 8 mm. With increasing width t, enhanced bandwidth of the lower band is obtained. An additional higher-order loop resonant mode at about 2.7 GHz contributed by shorted strip 1 can also be excited with a widened portion of $t = 6$ or 8 mm, which enhances the bandwidth of the upper band.

Simulated surface current distributions on the major metal pattern of the antenna are presented in Fig. 12. From the surface current distribution at 740 MHz, it is seen that the coupled-fed loop on the left-hand side formed by arm 1 and shorted strip 1 is excited at its fundamental mode and there is no current null along the resonant path. Similar results are seen at 1000 MHz for the coupled-fed loop on the right-hand side formed by arm 2 and shorted strip 2. The results confirm that the two separate quarter-wavelength resonant modes [37] are excited to form a

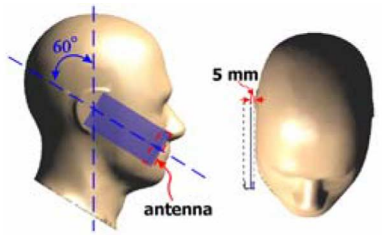

Frequency (MHz)	Testing power (dBm)	SAR (W/kg)	Return loss (dB)
740	21	0.54	8.7
859	24	1.01	5.6
925	24	1.11	6.2
1795	21	0.70	14.1
1920	21	0.57	15.1
2045	21	0.47	11.2
2350	21	0.66	22.0
2595	21	0.62	7.6

Fig. 13. SAR simulation model and the simulated SAR values for 1-g tissue for the proposed antenna.

wide lower band for the antenna. While at 1940 and 2350 MHz, strong surface current distributions on arm 1 and arm 2 are seen, which agrees with the discussion in Fig. 8. At 2700 MHz, the surface current distribution agrees with the observation in Fig. 7, in which the resonant mode at about 2700 MHz is related to a higher-order resonant mode of the coupled-fed loop on the left-hand side.

In addition, for practical applications, the SAR values of the antenna should be less than 1.6 W/kg for 1-g head tissue [9]. To analyze the SAR results, Fig. 13 shows the SAR simulation model and the simulated SAR values for 1-g head tissue for the antenna. In the simulation model, the typical parameters of the head phantom liquid are $\varepsilon_r = 41.5$, $\sigma = 0.97\ (\mathrm{S/m})$ at 900 MHz, and $\varepsilon_r = 40$, $\sigma = 1.4\ (\mathrm{S/m})$ at 1800 MHz. The simulated results are obtained using the SPEAG simulation software SEMCAD X version 14 [38]. The main circuit board with the antenna mounted at the bottom is placed close to the head phantom with a 5-mm distance to simulate the thickness of the handset housing. At each testing frequency (central frequencies of the eight operating bands), the SAR values are tested using input power of 24 dBm for the GSM850/900 (859, 925 MHz) system and 21 dBm for the GSM1800/1900/UMTS (1795, 1920, 2045 MHz) and LTE700/2300/2500 (740, 2350, 2595 MHz) systems [39]–[41]. The return loss given in the table shows the impedance matching level at the testing frequency. The obtained SAR values are well below the SAR limit of 1.6 W/kg, indicating that the antenna is promising for practical handset applications.

IV. Conclusion

A promising internal eight-band WWAN/LTE antenna integrated with a USB connector at the bottom edge of the mobile handset has been proposed. The antenna is mounted above a protruded ground extended from the main ground plane of the handset, which allows the antenna to integrate with a USB connector disposed on the protruded ground. Further, two coupled-fed loop resonant paths capable of generating quarter-wavelength modes have been provided by the antenna. The proposed design makes the antenna not only capable of WWAN/LTE operation but also suitable to integrate nearby associated elements such as a USB connector at the bottom edge as the data port of the handset. Good far-field radiation characteristics for frequencies over the eight operating bands have also been observed. Acceptable near-field emission of the antenna with its SAR values for 1-g head tissue well less than 1.6 W/kg has been obtained. From the results shown in this study, the proposed antenna is promising for practical applications in a smartphone for eight-band WWAN/LTE operation.

References

[1] F. H. Chu and K. L. Wong, "Simple planar printed strip monopole with a closely-coupled parasitic shorted strip for eight-band LTE/GSM/UMTS mobile phone," *IEEE Trans. Antennas Propag.*, vol. 58, no. 10, pp. 3426–3431, Oct. 2010.

[2] C. T. Lee and K. L. Wong, "Planar monopole with a coupling feed and an inductive shorting strip for LTE/GSM/UMTS operation in the mobile phone," *IEEE Trans. Antennas Propag.*, vol. 58, no. 7, pp. 2479–2483, Jul. 2010.

[3] S. C. Chen and K. L. Wong, "Small-size 11-band LTE/WWAN/WLAN internal mobile phone antenna," *Microwave Opt. Technol. Lett.*, vol. 52, pp. 2603–2608, Nov. 2010.

[4] K. L. Wong, W. Y. Chen, C. Y. Wu, and W. Y. Li, "Small-size internal eight-band LTE/WWAN mobile phone antenna with internal distributed *LC* matching circuit," *Microwave Opt. Technol. Lett.*, vol. 52, pp. 2244–2250, Oct. 2010.

[5] K. L. Wong, M. F. Tu, C. Y. Wu, and W. Y. Li, "Small-size coupled-fed printed PIFA for internal eight-band LTE/GSM/UMTS mobile phone antenna," *Microwave Opt. Technol. Lett.*, vol. 52, pp. 2123–2128, Sep. 2010.

[6] S. C. Chen and K. L. Wong, "Bandwidth enhancement of coupled-fed on-board printed PIFA using bypass radiating strip for eight-band LTE/GSM/UMTS slim mobile phone," *Microwave Opt. Technol. Lett.*, vol. 52, pp. 2059–2065, Sep. 2010.

[7] K. L. Wong and W. Y. Chen, "Small-size printed loop-type antenna integrated with two stacked coupled-fed shorted strip monopoles for eight-band LTE/GSM/UMTS operation in the mobile phone," *Microwave Opt. Technol. Lett.*, vol. 52, pp. 1471–1476, Jul. 2010.

[8] C. W. Chiu, C. H. Chang, and Y. J. Chi, "A meandered loop antenna for LTE/WWAN operations in a smart phone," *Progr. Electromagn. Rese. C*, vol. 16, pp. 147–160, 2010.

[9] *Safety Levels With Respect to Human Exposure to Radio-Frequency Electromagnetic Field, 3 kHz to 300 GHz*, ANSI/IEEE standard C95.1, 1999.

[10] C. H. Li, E. Ofli, N. Chavannes, and N. Kuster, "Effects of hand phantom on mobile phone antenna performance," *IEEE Trans. Antennas Propag.*, vol. 57, no. 9, pp. 2763–2770, Sep. 2009.

[11] Y. W. Chi and K. L. Wong, "Quarter-wavelength printed loop antenna with an internal printed matching circuit for GSM/DCS/PCS/UMTS operation in the mobile phone," *IEEE Trans. Antennas Propag.*, vol. 57, no. 9, pp. 2541–2547, Sep. 2009.

[12] C. H. Chang and K. L. Wong, "Printed $\lambda/8$-PIFA for penta-band WWAN operation in the mobile phone," *IEEE Trans. Antennas Propag.*, vol. 57, no. 5, pp. 1373–1381, May 2009.

[13] K. L. Wong and S. C. Chen, "Printed single-strip monopole using a chip inductor for penta-band WWAN operation in the mobile phone," *IEEE Trans. Antennas Propag.*, vol. 58, no. 3, pp. 1011–1014, Mar. 2010.

[14] Wikipedia, the Free Encyclopedia Universal Serial Bus [Online]. Available: http://en.wikipedia.org/wiki/Universal_Serial_Bus

[15] K. L. Wong, Y. W. Chang, C. Y. Wu, and W. Y. Li, "A small-size penta-band WWAN antenna integrated with USB connector for mobile phone applications," in *Proc. 2010 Int. Conf. Appl. Electromagn. Student Innovation Competition Awards*, Taipei, Taiwan, Aug. 11–13, 2010.

[16] K. L. Wong and C. H. Chang, "On-board small-size printed monopole antenna integrated with USB connector for penta-band WWAN mobile phone," *Microwave Opt. Technol. Lett.*, vol. 52, pp. 2523–2527, Nov. 2010.

[17] C. L. Liu, Y. F. Lin, C. M. Liang, S. C. Pan, and H. M. Chen, "Miniature internal penta-band monopole antenna for mobile phones," *IEEE Trans. Antennas Propag.*, vol. 58, no. 3, pp. 1008–1011, Mar. 2010.
[18] H. Rhyu, J. Byun, F. J. Harackiewicz, M. J. Park, K. Jung, D. Kim, N. Kim, T. Kim, and B. Lee, "Multi-band hybrid antenna for ultrathin mobile phone applications," *Electron. Lett.*, vol. 45, pp. 7730774–7730774, Jul. 2009.
[19] C. W. Chiu and Y. J. Chi, "Planar hexa-band inverted-F antenna for portable device applications," *IEEE Antennas Wireless Propag. Lett.*, vol. 8, no. 3, pp. 1099–1102, Mar. 2009.
[20] R. A. Bhatti, Y. T. Im, J. H. Choi, T. D. Manh, and S. O. Park, "Ultrathin planar inverted-F antenna for multistandard handsets," *Microwave Opt. Technol. Lett.*, vol. 50, pp. 2894–2897, Nov. 2008.
[21] S. Hong, W. Kim, H. Park, S. Kahng, and J. Choi, "Design of an internal multiresonant monopole antenna for GSM900/DCS1800/US-PCS/S-DMB operation," *IEEE Trans. Antennas Propag.*, vol. 56, no. 5, pp. 1437–1443, May 2008.
[22] S. Y. Lin, "Multiband folded planar monopole antenna for mobile handset," *IEEE Trans. Antennas Propag.*, vol. 52, pp. 1790–1794, Jul. 2004.
[23] K. L. Wong, *Planar Antennas for Wireless Communications*. New York: Wiley, 2003.
[24] Y. W. Chi and K. L. Wong, "Very-small-size printed loop antenna for GSM/DCS/PCS/UMTS operation in the mobile phone," *Microwave Opt. Technol. Lett.*, vol. 51, pp. 184–192, Jan. 2009.
[25] Y. W. Chi and K. L. Wong, "Internal compact dual-band printed loop antenna for mobile phone application," *IEEE Trans. Antennas Propag.*, vol. 55, no. 5, pp. 1457–1462, May 2007.
[26] Y. W. Chi and K. L. Wong, "Compact multiband folded loop chip antenna for small-size mobile phone," *IEEE Trans. Antennas Propag.*, vol. 56, pp. 3797–3803, Dec. 2008.
[27] Y. W. Chi and K. L. Wong, "Half-wavelength loop strip fed by a printed monopole for penta-band mobile phone antenna," *Microwave Opt. Technol. Lett.*, vol. 50, pp. 2549–2554, Oct. 2008.
[28] Y. W. Chi and K. L. Wong, "Very-small-size folded loop antenna with a band-stop matching circuit for WWAN operation in the mobile phone," *Microwave Opt. Technol. Lett.*, vol. 51, pp. 808–814, Mar. 2009.
[29] K. L. Wong and C. H. Huang, "Printed loop antenna with a perpendicular feed for penta-band mobile phone application," *IEEE Trans. Antennas Propag.*, vol. 56, pp. 2138–2141, Jul. 2008.
[30] B. K. Yu, B. Jung, H. J. Lee, F. J. Harackiewwicz, and B. Lee, "A folded and bent internal loop antenna for GSM/DCS/PCS operation of mobile handset applications," *Microwave Opt. Technol. Lett.*, vol. 48, pp. 463–467, Mar. 2006.
[31] B. Jung, H. Rhyu, Y. J. Lee, F. J. Harackiewwicz, M. J. Park, and B. Lee, "Internal folded loop antenna with tuning notches for GSM/GPS/DCS/PCS mobile handset applications," *Microwave Opt. Technol. Lett.*, vol. 48, pp. 1501–1504, Aug. 2006.
[32] Y. L. Kuo and K. L. Wong, "Printed double-T monopole antenna for 2.4/5.2 GHz dual-band WLAN operations," *IEEE Trans. Antennas Propag.*, vol. 51, pp. 2187–2192, Sep. 2003.
[33] Ansoft Corporation HFSS [Online]. Available: http://www.ansoft.com/products/hf/hfss/
[34] H. W. Hsieh, Y. C. Lee, K. K. Tiong, and J. S. Sun, "Design of a multiband antenna for mobile handset operations," *IEEE Antennas Wireless Propag. Lett.*, vol. 8, pp. 200–203, 2009.
[35] X. Zhang and A. Zhao, "Bandwidth enhancement of multiband handset antennas by opening a slot on mobile handset," *Microwave Opt. Technol. Lett.*, vol. 51, pp. 1702–1706, Jul. 2009.
[36] C. L. Liu, Y. F. Lin, C. M. Liang, S. C. Pan, and H. M. Chen, "Miniature internal penta-band monopole antenna for mobile phones," *IEEE Trans. Antennas Propag.*, vol. 58, no. 3, pp. 1008–1011, Mar. 2010.
[37] K. L. Wong, W. Y. Chen, and T. W. Kang, "On-board printed coupled-fed loop antenna in close proximity to the surrounding ground plane for penta-band WWAN mobile phone," *IEEE Trans. Antennas Propag.*, vol. 59, no. 3, pp. 751–757, Mar. 2011.
[38] SEMCAD Schmid & Partner Engineering AG (SPEAG) [Online]. Available: http://www.semcad.com
[39] "Technical Specification Group GSM/EDGE Radio Access Network; Radio Transmission and Reception (Release 9)," 3rd Generation Partnership Project (3GPP), *3GPP, TS 45.005 V9.5.0* 2010.
[40] "Technical Specification Group Radio Access Network; Terminal conformance specification; Radio transmission and reception (FDD) (Release 6)," 3rd Generation Partnership Project (3GPP), *3GPP, TS 34.121 V6.3.0* 2005.
[41] "Technical Specification Group Radio Access Network; Evolved Universal Terrestrial Radio Access (E-UTRA); User Equipment (UE) radio transmission and reception (Release 9)," 3rd Generation Partnership Project (3GPP), *3GPP, TS 36.101 V9.0.0* 2009.

Fang-Hsien Chu (S'11) was born in Kaohsiung, Taiwan, in 1983. He received the B.S. degree in electronic communication engineering from National Kaohsiung Marine University, Kaohsiung, Taiwan, in 2005, and the M.S. degree in photonics and communications from National Kaohsiung University of Applied Sciences, Kaohsiung, Taiwan, in 2007. He is currently working toward the Ph.D. degree at National Sun Yat-Sen University, Kaohsiung, Taiwan.

His main research interests are in planar antennas for wireless communications, especially for the planar antennas for mobile devices applications, and also in microwave and RF circuit design. Mr. Chu was awarded the second prize at the National Mobile Handset Antenna Design Competition in Taiwan in 2008.

Kin-Lu Wong (M'91–SM'97–F'07) received the B.S. degree in electrical engineering from National Taiwan University, Taipei, Taiwan, and the M.S. and Ph.D. degrees in electrical engineering from Texas Tech University, Lubbock, TX, in 1981, 1984, and 1986, respectively.

From 1986 to 1987, he was a visiting scientist with Max-Planck-Institute for Plasma Physics in Munich, Germany. Since 1987 he has been with the Department of Electrical Engineering, National Sun Yat-Sen University (NSYSU), Kaohsiung, Taiwan, where he became a Professor in 1991. From 1998 to 1999, he was a Visiting Scholar with the ElectroScience Laboratory, The Ohio State University, Columbus, OH. In 2005, he was elected to be Sun Yat-sen Chair Professor of NSYSU. He also served as Chairman of the Electrical Engineering Department from 1994 to 1997, Dean of the Office of Research Affairs from 2005 to 2008, and now as Vice President for Academic Affairs, NSYSU. He has published more than 500 refereed journal papers and 250 conference articles and has personally supervised 50 graduated Ph.Ds. He also holds over 100 patents, including U.S., Taiwan, China, EU patents, and has many patents pending. He is the author of *Design of Nonplanar Microstrip Antennas and Transmission Lines* (Wiley, 1999), *Compact and Broadband Microstrip Antennas* (Wiley, 2002), and *Planar Antennas for Wireless Communications* (Wiley, 2003).

Dr. Wong is an IEEE Fellow and received the Outstanding Research Award three times from National Science Council of Taiwan in 1995, 2000 and 2002, and was elevated to be a Distinguished Research Fellow of National Science Council in 2005. He also received the Outstanding Research Award from NSYSU in 1995, the ISI Citation Classic Award for a published paper highly cited in the field in 2001, the Outstanding Electrical Engineer Professor Award from Institute of Electrical Engineers of Taiwan in 2003, and the Outstanding Engineering Professor Award from Institute of Engineers of Taiwan in 2004. In 2008, the research achievements of handheld wireless communication devices antenna design of NSYSU Antenna Lab that he led was selected to be one of the top 50 scientific achievements of National Science Council of Taiwan in past 50 years (1959–2009). He was awarded the 2010 Outstanding Research Award of Pan Wen Yuan Foundation and selected as top 100 honor of Taiwan by Global Views Monthly in August 2010 for his contribution in mobile communication antenna researches. He was also awarded the Best Paper Award (APMC Prize) in 2008 Asia-Pacific Microwave Conference held in Hong Kong, China. His graduate students were the winners of Best Student Paper Awards in 2008 APMC, 2009 ISAP, and 2010 ISAP (International Symposium on Antennas and Propagation). His graduate students also won the first prize of 2007 and 2009 Taiwan National Mobile Handset Antenna Design Competition.